Brownian motion in quasibidimensional colloidal suspensions

M. D. Carbajal-Tinoco, G. Cruz de León, and J. L. Arauz-Lara
Instituto de Física ''Manuel Sandoval Vallarta,'' Universidad Autónoma de San Luis Potosí, Alvaro Obregón 64, 78000 San Luis Potosí, SLP, Mexico

(Received 18 April 1997; revised manuscript received 10 July 1997)

Digital video microscopy is used to study the Brownian motion in quasibidimensional colloidal systems, consisting of spherical polystyrene particles suspended in water and confined between two glass plates. This technique allows the direct measurement of the lateral (two-dimensional) probability distribution function, $P(\Delta\mathbf{r},t)$, of the random variable $\Delta\mathbf{r}$ (the particle displacement) at time t, and the mean squared displacement $W(t)$. We studied the effect of confinement in highly diluted samples, where $W(t)$ is found to be a linear function of time. The hydrodynamic interactions between the colloidal particles and the glass walls are found to be more important than predicted by approximate hydrodynamic theories. Keeping fixed the separation between the plates, we studied the effect of direct and hydrodynamic interactions between the particles by increasing the particle concentration. In this case, the short time dynamics is characterized by means of a theoretical approach that describes self-diffusion in terms of the static structure of the suspension. In all the samples studied, we found negligible deviations of $P(\Delta\mathbf{r},t)$ from Gaussian behavior. [S1063-651X(97)00512-6]

PACS number(s): 82.70.Dd, 05.40.+j

I. INTRODUCTION

Single particle motion of submicron size particles suspended in a fluid, commonly referred to as Brownian motion or self-diffusion, is a fascinating phenomenon, paradigm of the stochastic processes, whose description for noninteracting particles can be found in various statistical mechanics and colloidal physics text books [1,2]. Briefly, the simplest quantity describing Brownian motion is the mean squared displacement, $W(t)\equiv\langle[\mathbf{r}(t)-\mathbf{r}(0)]^2\rangle/2$ dim, where $\mathbf{r}(t)$ is the position of the particle at time t, dim is the system's dimensionality, and the angular parentheses indicate equilibrium ensemble average. For isotropic systems we can write $W(t)$ in terms of the displacement along only one direction, say x, i.e.,

$$W(t)=\langle[x(t)-x(0)]^2\rangle/2. \tag{1.1}$$

For noninteracting particles (i.e., in the limit of infinite dilution) in a homogeneous three-dimensional (3D) suspension, $W(t)$ is a linear function of time, i.e.,

$$W(t)=D_0 t \tag{1.2}$$

in the diffusive time regime, defined by $t\gg\tau_B\equiv M/\zeta$, where M and ζ are the particle mass and the translational friction coefficient, respectively. The slope D_0 of the mean squared displacement is the free-particle self-diffusion coefficient given by the Einstein relation, $D_0=k_BT/\zeta$, where k_BT is the thermal energy. For a spherical particle of diameter d with stick boundary conditions the friction coefficient is $\zeta=3\pi\eta d$, with η being the shear viscosity of the solvent. Deviations from Eq. (1.2) are due to the particles' interactions, hydrodynamic and direct, with the surroundings (other particles at finite concentration, external fields, constraining boundaries, etc.).

For the last two decades, self-diffusion has been studied (theoretically, experimentally, and by computer simulations) mostly in the bulk, i.e., in homogeneous 3D colloidal systems where the properties of $W(t)$ are determined only by the (direct and hydrodynamic) interactions between the particles [3,4]. However, in many cases of interest one is concerned with the motion of Brownian particles (proteins, polymers, colloidal particles, etc.) in restricted geometries (near a wall or between two of them, in a capillary, inside a cell, in a polymeric solution, etc.), where the interactions, also direct and hydrodynamic, between the particles and the surroundings are now quite important to determine their motion. Thus, in this work we study the Brownian motion of colloidal particles in a quasi-two-dimensional system by means of digital video microscopy (DVM). Our system consists of fluorescent polystyrene spheres of diameter $d=0.5$ μm, suspended in water and confined between two parallel glass plates, forming a quasibidimensional system. We investigate on one hand the effect of confinement on the lateral motion by varying the separation between the plates, keeping the particle concentration very low such that the interactions between particles are negligible. Thus, $W(t)$ is only affected by the hydrodynamic coupling and the direct interactions between the particles and the walls. On the other hand, for fixed plates separation, we varied the particle concentration so that the interactions between particles are also important. Let us mention that some recent studies, by DVM and by evanescent wave dynamic light scattering (EWDLS), of Brownian motion on similar systems to ours have been reported in the literature [5–8]. In Ref. [5] the authors address the problem of determining the particle concentration dependence of the self-diffusion coefficient of hard spheres, of diameter ~ 0.5 μm at fixed plates separation of about three times the particles diameter, and various plates separations in the case of highly dilute samples. Although the work reported in [5] seems similar to ours, two main differences should be noted. First, the interactions between the particles

in our systems are not (only) hard spheres (see our discussion in Sec. III). Second, we study the time dependence of $W(t)$ with an experimental time resolution of 1/30 s. In [5] the time resolution is 0.25 s (about one order of magnitude larger). Therefore, we study a qualitatively different set of systems at a shorter time scale, so that we look closer into the short-time regime. In Refs. [6,7], the authors focus their attention on the motion of isolated large particles ($d \geqslant 1\ \mu$m) and large separations between the plates. Although some cases considered in [7] are similar to our systems in terms of the plates separation to particle diameter ratio, they study only isolated spheres and do not consider the particle concentration dependence. In [8] the authors study the Brownian motion in a suspension of hard spheres, of diameter 1 μm and plates separation of 3 μm, using DVM and EWDLS. Here, again, the interparticle potential is different from our case. Since only one system is considered in [8], the dependence on plates separation and particle concentration is not determined.

In the following sections we discuss some details corresponding to the sample preparation and the detection of particle trajectories (Sec. II), then we present and discuss our results (Sec. III), and in Sec. IV we summarize our findings. However, before going into the details, let us sketch some general aspects of the Brownian motion in the bulk, so that it might provide some general basis to understand Brownian motion in the case considered here. For 3D suspensions, as we mentioned before, $W(t)=D_0 t$ in the limit of infinite dilution. At finite concentrations, the mean squared displacement is a linear function of time only in the short and in the long time regimes, with different proportionality constants [3], i.e.,

$$W(t)=\begin{cases} D_S t, & t \lesssim t_0 \sim d^2/D_0 \\ D_L t, & t \gg t_I \sim l^2/D_0, \end{cases} \tag{1.3}$$

with $D_L \leqslant D_S \leqslant D_0$, and with l being the mean interparticle distance. The deviation of D_S, the short-time self-diffusion coefficient, from its low concentration value D_0 reflects the effect of the hydrodynamic coupling between particles on their Brownian motion, and it depends only on the volume fraction ϕ occupied by the macroparticles. Theoretical calculations and experimental results for D_S as a function of ϕ are reported in the literature [3,9]. On the other hand, the value of D_L, the long-time self-diffusion coefficient, contains the effect of both direct (electrostatic, excluded volume, etc.) and hydrodynamic interactions between particles. Thus, the initial increase of $W(t)$ is linear, with slope D_S, and then it deviates from this behavior due to the direct interactions of the tracer particle with its neighbors, and at long times it is again linear with slope D_L. Due to the large difference in the characteristic time scales of the hydrodynamic and direct interactions, their contributions on the Brownian motion of single particles can be decoupled [10,11]. This means that the mean squared displacement can be expressed as $W(t)=W_I(t)D_S/D_0$, where $W_I(t)$ is the mean squared displacement of particles with the same direct interactions, but hydrodynamically uncoupled. Calculations from theoretical approaches that express $W_I(t)$ in terms of microscopic quantities of the system, such as the pair potential between colloidal particles $u(r)$, the particle concentration, etc., and the static properties such as the radial distribution function or the static structure factor, have been reported to describe accurately the experimental and computer simulation data for $W_I(t)$, obtained from dilute suspensions of strongly interacting colloidal particles, such as polystyrene spheres in water [12–14].

II. EXPERIMENTAL DETAILS

A. System preparation

A colloidal suspension of fluorescent polystyrene spheres of diameter $d=0.5\pm0.015\ \mu$m (Duke Scientific) is dispersed and diluted in ultrapure water (Barnstead). The suspension is dialyzed to reduce the ionic concentration and the excess of dissolved surfactants from the original batch. The systems studied are prepared as follows: in a clean atmosphere of nitrogen gas, a tiny volume of suspension ($\approx 0.5\ \mu$l) is confined between two carefully cleaned glass plates (a slide and a cover slip), which are uniformly pressed until a single layer of beads is obtained. The separation between the glass plates is accurately controlled by previously adding in the suspension a small amount of spheres with larger diameters (from 1 to 2.9 μm) that serve as spacers. Finally, the system is sealed with epoxy resin (Epo-Tek 302) to avoid any further contamination, especially from airborne CO_2. By carefully controlling the volume of suspension used in each sample, we avoid the contact with the epoxy resin and this prevents any contamination from the solvents. The sample is allowed to equilibrate for 1 or 2 days at a constant temperature of 23 °C (in contact with a circulating bath). The systems prepared with this procedure remain stable for several weeks or even months.

B. Digital video microscopy

Digital video microscopy is now a standard technique. In our case, we observe the sample through a fluorescence microscope (Zeiss Axioskop) with a 100× oil immersion objective (numerical aperture of 1.3). The motion of the particles is recorded by a charge-coupled device (CCD) video camera with a shutter exposure time of 1/250 s, attached to the microscope and connected to a video tape recorder (Hi8 Sony EV-100). The images are then digitized using a frame grabber with a resolution of 640×480 pixel^2 (Data Translation). With this setup, we measure 1 μm=16.7 pixel.

C. Tracking particles

Although in our samples there is enough room for the particles to move in the direction perpendicular to the plates, we observed in all cases very little vertical motion, i.e., the particles' vertical motion was never large enough to move them out of focus. Let us mention, however, that for higher concentrations than those studied here (see Table I), the vertical motion is larger and the particles can move out of focus. This effect is more pronounced for large plates separations ($\gtrsim 3\ \mu$m). The positions of the particles along the lateral plane of motion are determined from the digitized images by using the method deviced by Crocker and Grier [15], which allows one to locate the spheres' centroids with a precision of 1/5 pixel ($\sim 0.02d$). The trajectories of the particles are reconstructed from the particles' positions at consecutive

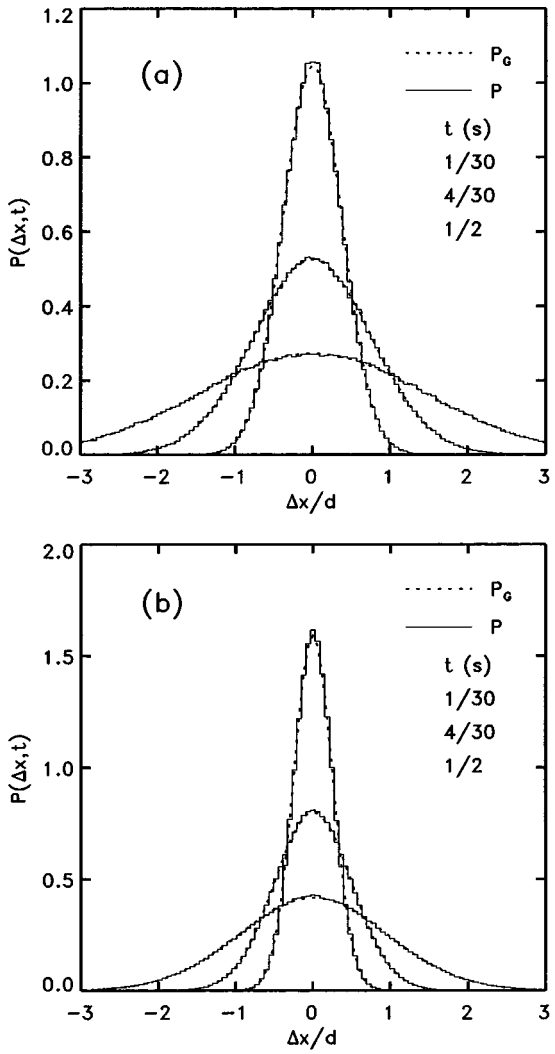

FIG. 1. Normalized probability distribution functions $P(\Delta x,t)$ of the random variables $\Delta x=x(t)-x(0)$ (the displacement of Brownian particles during a time t). Distribution functions (solid lines) corresponding to particles in samples A and E are shown in (a) and (b), respectively, for three different times. For comparison, the Gaussian functions $P_G(\Delta x,t)$, constructed with the mean value and variance of the experimental distribution functions, are also shown (dashed lines).

frames, with a time resolution of 1/30 s, in the following way. We first notice that the largest displacement of the particles between two consecutive frames was observed to be less than $1.5d$ [see Fig. 1(a)]. As the initial step, we identify the positions $\mathbf{r}_i(0)$ of the particles, which in the first frame ($t=0$) are isolated, i.e., particles that do not have any neighbor closer than $3d$. Thus, in the second frame ($t=\Delta t=1/30$ s) there will be only one particle whose position $\mathbf{r}(\Delta t)$ satisfies the condition $|\mathbf{r}(\Delta t)-\mathbf{r}_i(0)|\leq 1.5d$, we then take $\mathbf{r}_i(\Delta t)=\mathbf{r}(\Delta t)$. We then search for the particles i in the first frame that do have just one neighbor at a distance between $1.5d$ and $3d$, and we look for the particles in the second frame whose positions satisfy $|\mathbf{r}(\Delta t)-\mathbf{r}_i(0)|\leq 1.5d$. If only one particle is found, it is particle i; if there are two, we calculate the distance between the particles of the two possible configurations from frame 1 to frame 2. We choose the configuration leading to the lower value of the total distance between particles. We consider more complex situations (particles with two neighbors, etc.) until the positions $\mathbf{r}_i(\Delta t)$ are completely identified. In each step, the particles already identified are removed so that they are not considered in the next step. This procedure is then applied to frames 2 and 3, and so on. The trajectories of the particles that leave or enter the observation region during the time interval analyzed are not considered. For concentrated systems, this method of tracking particles may interchange their trajectories. For this reason, in this work we restrict ourselves to the analysis of the Brownian motion only in dilute and semidilute systems. Table I summarizes the characteristics of the 5 samples studied. For each system, several runs of 750 consecutive frames were digitized and the particles' trajectories determined.

TABLE I. Here we summarize the experimental conditions for the 5 samples studied. The glass plate separation is given by h, the reduced concentration by $n^*=nd^2$ with n the average number of particles per unit area observed in a frame, D_s is the measured short-time self-diffusion coefficient (see Sec. IV) and $D_0=0.923\ \mu\text{m}^2/\text{s}$ (calculated from the Einstein relation).

Sample	A	B	C	D	E
h (μm)	2.9	2.0	1.0	1.0	1.0
n^*	0.007	0.006	0.006	0.046	0.080
D_s/D_0	0.58	0.42	0.39	0.35	0.26

III. RESULTS AND DISCUSSION

The fundamental quantity describing Brownian motion is the normalized probability distribution function $P(\Delta\mathbf{r},t)$ of single particle displacements $\Delta\mathbf{r}=\mathbf{r}(t)-\mathbf{r}(0)$, during a time t [16]. As we have already mentioned, the properties of the Brownian motion are usually discussed in terms of a more simple quantity, namely, the mean squared displacement $W(t)$, which is nothing but the second moment of $P(\Delta\mathbf{r},t)$, i.e.,

$$W(t)=\frac{1}{2\text{dim}}\int d\mathbf{r}(\Delta\mathbf{r})^2P(\Delta\mathbf{r},t). \tag{3.1}$$

With the trajectories of the particles available, we can calculate $P(\Delta\mathbf{r},t)$, as well as other relevant quantities. If the orthogonal directions x and y defining the plane of motion are independent, then $P(\Delta\mathbf{r},t)=P(\Delta x,t)P(\Delta y,t)$, with $P(\Delta x,t)$ and $P(\Delta y,t)$ being the normalized probability distribution functions of displacements along the directions x and y, respectively, at time t. To calculate these functions we choose discrete intervals of size 1 pixel ($\sim 0.1d$) and count the number of displacements $\Delta\mathbf{r}$, Δx, and Δy at time t whose values fall within each interval. The normalized functions are obtained by dividing the histograms by the total number of events considered, which in all the samples studied here were of order 10^5-10^6, so that there are enough data to average out statistical fluctuations, thus obtaining smooth functions. Furthermore, in a homogeneous 2D system in thermal equilibrium, it should happen that $P(\Delta x,t)=P(\Delta y,t)$. This is in fact what we found in our systems and also that $P(\Delta\mathbf{r},t)=P(\Delta x,t)P(\Delta y,t)$. Thus, it

is sufficient to discuss the results only for one of these functions. In Fig. 1 we show $P(\Delta x,t)$ (solid lines) for samples A [Fig. 1(a)] and E [Fig. 1(b)] (see Table I). As one can see in these figures, $P(\Delta x,t)$ are symmetric functions centered around $\Delta x=0$, and they spread out as time increases due to the diffusion of the particles. If the confinement is increased, by reducing the distance h between the plates and/or by increasing the particle concentration, the particles become less mobile and the distribution functions are narrower. In other words, since $P(\Delta x,t=0)=\delta(\Delta x)$ for all the samples, these functions spread slower for more confined systems due to the increased interactions of the particles with their surroundings. This effect can be seen in Fig. 1, where we show $P(\Delta x,t)$ for the least and most confined systems we studied.

In an isotropic system of noninteracting particles the distribution functions $P(\Delta x,t)$ are Gaussian functions centered around $\Delta x=0$ (i.e., with $\langle \Delta x\rangle=0$) and with dispersions $\sigma(t)\equiv\sqrt{\langle \Delta x^2(t)\rangle}=\sqrt{2D_0t}$ [1]. For 3D colloidal suspensions at finite concentrations, the interactions between the particles introduce negligible non-Gaussian corrections so that Gaussian functions with dispersions $\sigma(t)=\sqrt{2W(t)}$ are excellent approximations for the distribution functions [17]. Here we can ask the question: to what extent can the motion of Brownian particles under confinement still be described by Gaussian probability distribution functions? In our case, we can answer this question by quantifying the deviation of $P(\Delta x,t)$ from Gaussian behavior. For all the samples studied here, we obtained functions $P(\Delta x,t)$ that are similar to the histograms plotted in Fig. 1, i.e., they look very much like Gaussian functions and in fact one can make a nonlinear least squares fit to find the Gaussian function that best fits the experimental data for $P(\Delta x,t)$. However, we should proceed in a different and more rigorous way. From $P(\Delta x,t)$ or, more directly, from the trajectories of the particles, we can calculate the moments $\mu_l(t)\equiv\langle[x(t)-x(0)]^l\rangle$ of the distribution functions. With the first two moments we can construct normalized Gaussian functions $P_G(\Delta x,t)$ having the mean value and dispersion of the experimental distribution function, i.e.,

$$P_G(\Delta x,t)=\frac{1}{\sqrt{4\pi W(t)}}\exp\left[-\frac{\Delta x^2}{4W(t)}\right], \tag{3.2}$$

where $W(t)$ is the measured mean squared displacement. We have set $\mu_1(t)=0$ in Eq. (3.2), since for all the samples we found that $|\langle x(t)-x(0)\rangle|/d\sim10^{-3}-10^{-5}$. In Fig. 1 we plotted also the functions $P_G(\Delta x,t)$ (dashed lines), and we can see that they overlap the experimental functions. However, to have a more quantitative account of the extent of non-Gaussian behavior of $P(\Delta x,t)$, we look at the moments of higher order; μ_3, μ_4, etc. A customary way to characterize stochastic processes such as $\Delta x(t)$ is by looking at their characteristic functions $F_s(k,t)$, which are nothing but the Fourier transform of the distribution functions [16], i.e.,

$$F_s(k,t)=\int dx P(\Delta x,t)e^{-ik\Delta x}=\langle e^{-ik[x(t)-x(0)]}\rangle. \tag{3.3}$$

For the processes described by Eq. (3.2) we have

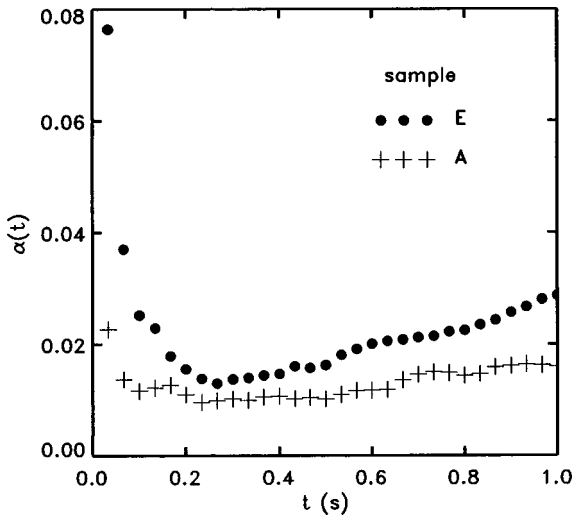

FIG. 2. Non-Gaussian parameter $\alpha(t)$ for samples A and E.

$$F_s^G(k,t)=e^{-k^2W(t)}. \tag{3.4}$$

In a more general way, Eq. (3.3) can be written as [3,17,18]

$$F_s(k,t)=e^{-k^2W(t)}\{1+\tfrac{1}{2}[k^2W(t)]^2\alpha(t)+\cdots\}, \tag{3.5}$$

where

$$\alpha(t)=\frac{\langle[x(t)-x(0)]^4\rangle}{3\langle[x(t)-x(0)]^2\rangle^2}-1 \tag{3.6}$$

is the leading term containing the non-Gaussian effects. In Fig. 2 we show a plot of $\alpha(t)$ for the samples in Fig. 1. For the other samples the values of this quantity lie below the curve for sample E (filled circles). Thus, the results plotted in Fig. 2 show that the non-Gaussian effects are more important for more confined systems, but within the ranges of h and n^* studied here they are very small. Therefore, the Gaussian approximation is a good approximation.

Let us now discuss in more detail the effect of the interactions between the particles. As mentioned before, the quantitative effect of the interactions on the Brownian motion is better visualized in terms of the mean squared displacement. Thus, in Fig. 3 we plot $W(t)$ for the 5 samples studied. In Fig. 3(a) the mean squared displacement (symbols) for three highly diluted samples [A, B, and C, with reduced concentrations $n^*\approx6\times10^{-3}$ (see Table I)] at different plates separations, $h\approx6d$, $4d$, and $2d$, are shown. Here we can see the effect of reducing one dimension. For comparison, in this figure we also plot the mean squared displacement corresponding to the free diffusion of our colloidal particles in a 3D suspension (dashed line) given by Eq. (1.2). As one can see, the reduction of one dimension has an appreciable effect on the lateral motion of the colloidal particles, which become less mobile as the particles are more confined. In this figure one can also appreciate that $W(t)$ for these three samples seems to increase linearly with time [as predicted by Eq. (1.2)], but with slope smaller than D_0, i.e.,

$$W(t)=D_st, \tag{3.7}$$

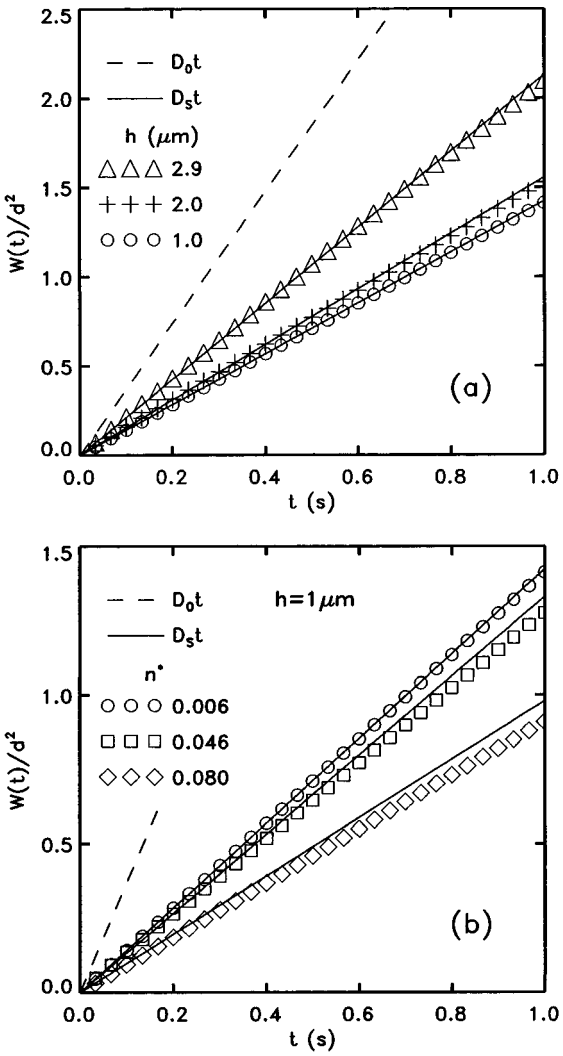

FIG. 3. Measured mean squared displacement vs time (symbols). In (a) we show the effect on $W(t)$ of reducing the distance between plates. In (b) we show the effect, at finite concentrations, of the direct and hydrodynamic interactions with other particles. The initial slopes (solid lines) are calculated using only the initial data points (a), and the FDA approximation (see text) (b). For comparison, we also plot $W(t)$ for a freely diffusing particle in 3D.

with $D_s<D_0$. Here we will refer to the slope D_s (as in 3D) as the short-time self-diffusion coefficient. Since the samples are highly dilute, the interactions between the particles are negligible. As we mention in the Introduction, in 3D suspensions at finite concentrations, the initial slope of the mean squared displacement is reduced from its free diffusion value D_0 due to the hydrodynamic interactions between the particles. Here we have also a reduction in the initial slope of $W(t)$, which in the absence of interactions with other particles, must be due to the effect of the hydrodynamic coupling and direct interactions between the particles and the confining walls. We can calculate the value of D_s by making a linear least squares fit to the experimental data for $W(t)$. In Fig. 3(a) the solid lines are straight lines obtained by fitting only the first few (4–5) data points. As we can see, these lines constructed with the initial points reproduce the experimental data in the whole time interval studied. The values obtained in this way are quoted in Table I. Theoretical calculations of the friction coefficient of a spherical particle near a plane wall show that it increases (in fact it diverges in both directions, parallel and perpendicular to the plane) as the distance between the wall and the particle decreases [2,19]. Thus, a decrease in the particles mobility in a confined geometry is expected. However, a direct quantitative comparison is not possible since, to our knowledge, there is not an equivalent result for the case where the spherical particle is not close to one wall, but confined between two of them. We can, however, compare our results with the theoretical calculations by assuming that the hydrodynamic effect from the walls is additive. In this way we found that the measured values for D_s are about 30–40 % lower than those obtained by the superposition assumption. Therefore, we found that the lateral motion of ''freely diffusing'' (i.e., in the infinite dilution limit) colloidal particles in a quasi-bidimensional geometry can still be characterized by a mean squared displacement given by a linear function of time with slope D_s [Eq. (3.7)], which is smaller than the calculated value from the superposition assumption of the hydrodynamic coupling with both confining walls.

Now, at finite concentrations we can expect, as in the 3D case, a further reduction of the slope of $W(t)$ as a result of the interactions, both hydrodynamic and direct, between the particles. Also, as in 3D, we can expect the value of D_s to decrease as the particle concentration increases, as a result of the increase of the hydrodynamic interactions with the other particles. We can even expect a time scale separation from ''short'' times, where $W(t)$ follows Eq. (3.7), to another linear regime at ''larger'' times, where $W(t)=D_L t$, with $D_L<D_s$. In Fig. 3(b) we plot $W(t)$ for three samples with increasing reduced concentration $n^*=0.006$, 0.046, and 0.080, but with the same separation $h=1\ \mu$m between the glass plates (samples C, D, and E, respectively). As expected, $W(t)$ increases more slowly as the particle concentration (and the interactions between particles) increases, and in fact we see a strong effect on $W(t)$. As we said before, this effect arises from hydrodynamic and direct interactions, so the question is: can we estimate the corresponding contributions from each of those interactions? And still another question is the following: is there a time scale separation as in 3D? Under the assumption (introduced for 3D suspensions by Medina-Noyola [10]) that the effects from the hydrodynamic interactions and direct interactions can be decoupled, i.e., that the hydrodynamic effects enter through a renormalization of the value of D_s, we can answer both questions by determining D_s from the data in Fig. 3(b). For sample C it has been done by taking only a few initial points, as we already explained. For the other two samples (D and E) this calculation is somewhat more involved. For these samples we found that the slope of $W(t)$ changes with time, and therefore it depends on which data points are used to calculate the slope. Since the slope changes, it is not clear how to calculate D_s, and therefore, to quantify in a precise way the dependence of D_s on the particle concentration. However, we could still take the value of the slope determined from the initial data points just as an estimate of D_s, then the difference between the measured $W(t)$ and $D_s t$ would be an estimate of the effect of the direct interactions. We can, however, use a different approach to calculate D_s as explained below.

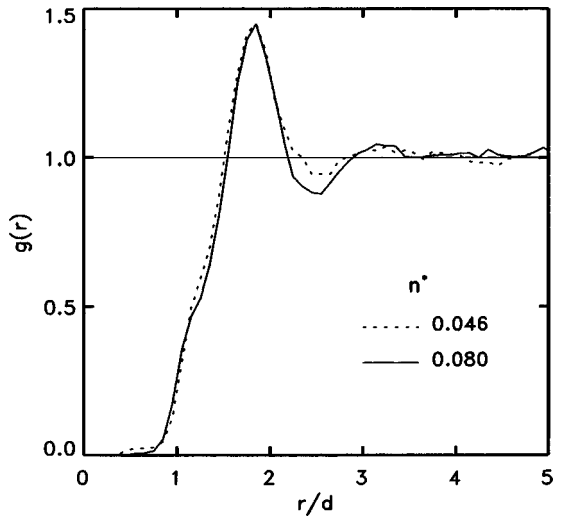

FIG. 4. Radial distribution functions corresponding to samples D ($n^*=0.046$) and E ($n^*=0.080$).

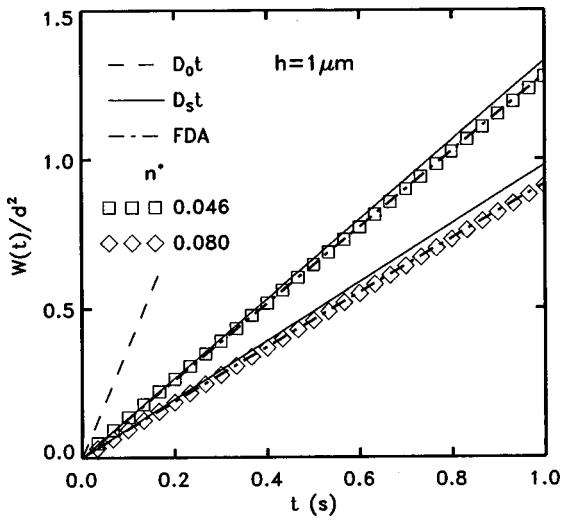

FIG. 5. $W(t)$ vs t for samples D and E (symbols). Dashed and solid lines are the results of FDA approximation for $W(t)$ and $D_s t$, respectively (see text).

In the case of 3D colloidal systems, theoretical approaches have been developed to describe colloidal dynamic properties, such as $W(t)$, in terms of static properties of the suspension. The accuracy of these theories has been established by comparing their predictions with experimental and computer simulation results for 3D [10,12–14] and the predictions of their 2D versions with computer simulations [21]. One of these theories, referred to as *Fick plus decoupling approximation* (FDA), has the appealing characteristic that, in order to calculate self-diffusion properties of interacting colloidal particles, it requires as input only static properties of the suspension and the short-time self-diffusion coefficient D_s. In this approach the effect of the direct interactions enters through the static structure, while the hydrodynamic effects are contained in the value of D_s.

Let us mention briefly the salient features of the FDA theory. It is based on the generalized Langevin equation

$$M\frac{d\mathbf{v}(t)}{dt}=-\zeta\mathbf{v}(t)+\mathbf{f}(t)-\int_0^t\Delta\zeta(t-t')\mathbf{v}(t')dt'+\mathbf{F}^{\mathrm{int}}(t), \tag{3.8}$$

where $\mathbf{v}(t)$ is the particle velocity, $\mathbf{f}(t)$ is a white random force, $\mathbf{F}^{\mathrm{int}}(t)$ is the colored random force exerted by the other particles on the labeled particle as their distribution departs instantaneously from its radial equilibrium average, and the kernel $\Delta\zeta(t)$ is a time-dependent friction function. The time-dependent correlation function of $\mathbf{F}^{\mathrm{int}}(t)$ is related to the (time-dependent) friction coefficient by a fluctuation-dissipation relation. The main result of the FDA is an expression for the time-dependent friction function $\Delta\zeta(t)$ in terms of static properties of the 2D suspension [21],

$$\Delta\zeta(t)=\frac{k_BTn}{4\pi}\int_0^\infty dk\,\frac{k^3h^2(k)}{1+nh(k)}e^{-k^2D_st\{1+1/[1+nh(k)]\}}. \tag{3.9}$$

This equation writes $\Delta\zeta(t)$ in terms of only $h(k)$ and D_s. The static property $h(k)$ is the Fourier transform of the total correlation function $h(r)=g(r)-1$, where $g(r)$ is the radial distribution function of particles around a central one [1,20]. The function $g(r)$ can be determined directly from the particles' positions [23]. In Fig. 4 we present $g(r)$ for samples D and E, from which the function $h(k)$ is obtained by a Fourier-Bessel transformation. From $\Delta\zeta(t)$, one can calculate self-diffusion properties such as the mean squared displacement, velocity autocorrelation function, and self-diffusion coefficient. Aranda-Espinoza *et al.* [21] discuss some details concerning the numerical procedure.

The FDA results for $W(t)$ are compared with the experimental data in Fig. 5. As we explained above, D_s is not accurately determined from the initial slope of $W(t)$. So, we use D_s as a fitting parameter in FDA, i.e., we choose the value of D_s that made the FDA and the experimental results coincide. Thus, here we use the theory in a rather different way, i.e., instead of using as an input $h(k)$ and D_s to get $W(t)$, we use $h(k)$ and $W(t)$ to get D_s. The values of D_s obtained from this procedure are slightly higher than the initial slope of $W(t)$, and they are used to draw the solid lines in Figs. 3(b) and 5, and are also quoted in Table I. Let us mention that the fitting of FDA to the experimental $W(t)$ is sensitive to D_s. For instance, a change of 2 or 3% in the value of D_s will make the FDA curve fall at long times ($\gtrsim 1$ s) out of the symbols representing the experimental data in Fig. 5. The relative uncertainty in the measured value of $W(t)$ is of order $N^{-1/2}$ [22], where N is the number of events averaged. In our case, as we mentioned above, $N\sim 10^5-10^6$. Thus, the relative uncertainty is $\sim 10^{-2}-10^{-3}$. On the other hand, the accuracy in the determination of the particles' position is $\sim 10^{-2}d$ (see Sec. II C). Therefore, error bars in our measurements of $W(t)$ are within the symbols in Figs. 3 and 5. Thus, differences in D_s of a few percent are important. If the FDA results are correct, two direct consequences should be noted. First, higher values of D_s than the initial slope of $W(t)$ mean that the interactions between the particles shift the short time regime to shorter times than the time resolu-

tion of our technique (0.033 s). Second, in Fig. 5 we see a significant decrease in $W(t)$ when the concentration increases. This decrease of $W(t)$ must be due to the (combined) effect of the increment of both the hydrodynamic and direct interactions between the particles, as a result of the increase in the concentration. Since, according to the FDA results, the direct interactions contribute only with a small part of the effect [compare $W(t)$ with $D_s t$], we may conclude that the hydrodynamic interactions should be responsible for most of the effect. The shift of the short time regime may be understood in terms of the particles direct interactions. In Fig. 4 we see that according to $g(r)$ the particles tend to be close to each other, and in fact there is strong evidence that, under confinement, the effective interparticle potential for polystyrene spheres in water has an attractive component around the position of the maximum of $g(r)$ [23–25]. Thus, at finite concentrations the first layer of neighbors is very close to the particle and the initial linear regime [Eq. (3.7)] only occurs at very short times. On the other hand, according also to Fig. 4, our systems are not highly structured (i.e., the direct interactions are not too strong). Thus, a small contribution from the direct interactions to $W(t)$ is reasonable. Thus, based on the FDA results, we can say that the hydrodynamic interactions between the particles are much stronger under confinement than in the bulk. For comparison, let us say that in the bulk $D_s/D_0 = 1 - 1.83\phi + O(\phi^2)$ in a suspension of spheres with volume fraction ϕ [9]. For samples D and E the corresponding volume fractions ($\phi = \pi n^* d/6h$, i.e., only taking into account the spheres and the solvent) are 0.012 and 0.021, respectively. Thus in 3D systems with these values of ϕ, the contribution to D_s from hydrodynamic interactions between the particles would be quite small.

Finally, and for completeness, let us note that in scattering experiments (dynamic light scattering in 3D and evanescent wave dynamic light scattering in quasi-2D) from colloidal suspensions, one measures the dynamic structure factor $F(k,t)$. This quantity describes the time evolution of local particle concentration fluctuations in Fourier space. For monodisperse systems with N particles,

$$F(k,t) = \frac{1}{N} \sum_{i,j=1}^{N} \langle \exp\{-i\mathbf{k}\cdot[\mathbf{r}_j(t) - \mathbf{r}_i(0)]\}\rangle. \quad (3.10)$$

For values of k where the static structure factor $S(k) \equiv F(k,t=0) = 1$, the cross terms ($i \neq j$) vanish and $F(k,t)$ reduces to its self-part ($i = j$) or self-dynamic structure factor, which then describes single particle dynamics in Fourier space. From Eqs. (3.3) and (3.10), and taking $\mathbf{k}$ in the direction of x, we see that the self-dynamic structure factor is nothing but the characteristic function $F_s(k,t)$. Thus, $W(t)$ can be obtained from light scattering experiments by applying the back Fourier transformation to the measured $F_s(k,t)$ and then using Eq. (3.1). In practice, a more economic way to obtain the mean squared displacement is by means of the Gaussian approximation [Eq. (3.4)]. For illustration, in Fig. 6 we show the self-dynamic structure factor corresponding to sample E, obtained from $P(\Delta x,t)$ through Eq. (3.3).

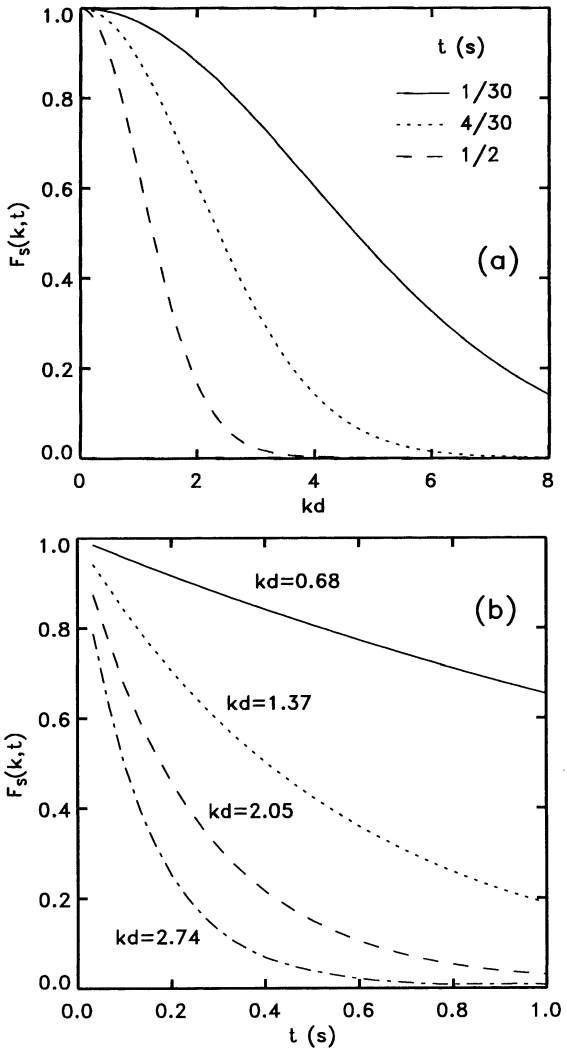

FIG. 6. Self-dynamic structure factor corresponding to sample E, shown as function of k (a) and time (b).

IV. CONCLUSIONS

In this work we studied the motion of colloidal particles in a quasibidimensional geometry. We presented experimental results for time-dependent quantities such as the mean squared displacement and the probability distribution function, along the effective plane of motion. The technique employed in this study, DVM, allows us to visualize directly the lateral motion of the particles. We considered highly dilute suspensions where the only effect on the particle motion arises from its interactions with the walls, which are found to be larger than predicted by approximate hydrodynamic theories. This point requires further theoretical investigation. For more concentrated samples, we also found that the hydrodynamic coupling between the particles induces a stronger effect than in the bulk and the effect of direct interactions on the particle motion can be described using the 2D version of a theoretical approach derived in the framework of 3D homogeneous suspensions. This approach was used to charac-

terize the short-time regime, which is apparently shifted to shorter times than our time resolution due to the specific (attractive) interactions between pairs of particles in our studied systems. We also found that, for all samples studied here, the probability distribution functions are very well approximated by Gaussian functions.

ACKNOWLEDGMENTS

We gratefully acknowledge helpful discussions with M. Medina-Noyola. This work was partially supported by the Consejo Nacional de Ciencia y Tecnología (CONACyT, Mexico), through Grant Nos. 3882E and I9109.

[1] D. A. McQuarrie, *Statistical Mechanics* (Harper and Row, New York, 1976).
[2] W. B. Russel, D. A. Saville, and W. R. Schowalter, *Colloidal Dispersions* (Cambridge University Press, Cambridge, 1989).
[3] P. N. Pusey, in *Liquids, Freezing and Glass Transition*, edited by J. P. Hansen, D. Levesque and J. Zinn-Justin (Elsevier, Amsterdam, 1991), p. 763.
[4] R. Klein and G. Nägele, Cur. Opin. Colloid Interface Sci. **1**, 4 (1996).
[5] W. Schaertl and H. Sillescu, J. Colloid Interface Sci. **155**, 313 (1993).
[6] N. A. Frej and D. C. Prieve, J. Chem. Phys. **98**, 7552 (1993).
[7] L. P. Faucheux and A. J. Libchaber, Phys. Rev. E **49**, 5158 (1994).
[8] A. H. Marcus, B. Lin, and S. A. Rice, Phys. Rev. E **53**, 1765 (1996).
[9] C. W. J. Beenakker and P. Mazur, Physica A **126**, 349 (1984).
[10] M. Medina-Noyola, Phys. Rev. Lett. **60**, 2705 (1988).
[11] J. F. Brady, Cur. Opin. Colloid Interface Sci. **1**, 472 (1996).
[12] J. L. Arauz-Lara and M. Medina-Noyola, J. Phys. A **19**, L117 (1986).
[13] G. Nägele, M. Medina-Noyola, R. Klein, and J. L. Arauz-Lara, Physica A **149**, 123 (1988).
[14] (a) R. Krauze, G. Nägele, D. Karrer, J. Schneider, R. Klein, and R. Weber, Physica A **153**, 400 (1988); (b) R. Krause, J. L. Arauz-Lara, G. Nägele, H. Ruiz-Estrada, M. Medina-Noyola, R. Weber, and R. Klein, *ibid.* **178**, 241 (1991).
[15] J. C. Crocker and D. G. Grier, J. Colloid Interface Sci. **179**, 298 (1996).
[16] N. G. van Kampen, *Stochastic Processes in Physics and Chemistry* (North-Holland, New York, 1981).
[17] W. van Megen and S. M. Underwood, J. Chem. Phys. **88**, 7841 (1988).
[18] J. P. Boon and S. Yip, *Molecular Hydrodynamics* (McGraw-Hill, New York, 1980).
[19] G. S. Perkins and R. B. Jones, Physica A **189**, 447 (1992).
[20] J. P. Hansen and I. R. McDonald, *Theory of Simple Liquids*, 2nd ed. (Academic Press, New York, 1986).
[21] H. Aranda-Espinoza, M. Carbajal-Tinoco, E. Urrutia-Bañuelos, J. L. Arauz-Lara, and M. Medina-Noyola, J. Chem. Phys. **101**, 10925 (1994).
[22] P. R. Bevington, *Data Reduction and Error Analysis for Physical Sciences* (McGraw-Hill, New York, 1969).
[23] M. D. Carbajal-Tinoco, F. Castro-Román, and J. L. Arauz-Lara, Phys. Rev. E **53**, 3745 (1996).
[24] G. M. Kepler and S. Fraden, Phys. Rev. Lett. **73**, 356 (1994).
[25] J. C. Crocker and D. G. Grier, Phys. Rev. Lett. **77**, 1897 (1996).